Analysis of the test condition of a shock-expansion tube: JF-16

Zongmin Hu*, Bo Wu, Zonglin Jiang

State Key Laborotary of High Temperature Gas Dynamics, Institute of Mechanics, CAS
No. 15, Beisihuanxi Road, Beijing, 100190, China

Abstract

A shock-expansion tube (SET, named JF-16) has been built at the State Key Laboratory of High Temperature Gas Dynamics (LHD) in order to generate relatively steady and clean test gas of really high enthalpy. However, the test time of a SET is extremely shorter as compared to a reflected-shock tunnel (RST) of the same scale which results in difficulties in the measurements and diagnostics. An applicable means to the flow diagnostics is the integrated computation-experiment techniques. In this paper, some numerical issues occurring in our computational investigation for the test flow of JF-16 are discussed. The dispersion-controlled dissipative scheme (DCD) is used to setup our SET simulation code. However, spurious oscillation at the contact surface occurs when the original scheme is applied to the simulation of JF-16 test flow. A new flux splitting algorithm based on local characteristics is worked out for the DCD scheme. Preliminary computations indicate that the updated algorithm is more robust to suppress the aforementioned oscillation as compared to the original algorithm. Several experiments with the typical hypervelocity test flow of JP-16 are computed and compared to validate the algorithms. The computations of double-wedge flows indicate that the experimental visualization is mainly the self-illumination of nitrogen atoms instead of the schlieren image.

Keywords: Shock-expansion tube; computation; spurious oscillation; flus splliting

1. Introduction

Reflected shock tunnels (RST) are the dominant ground test facilities to provide hypersonic test flows. However, severe challenges rise when RSTs are used for hypervelocity experiments where the test flow velocity may exceed 5 kmps. The contamination of the test gas and material erosion of the nozzle reservoir are the main issues among others. In addition, the frozen vibration energy or chemical species downstream of the nozzle throat of a RST may lead to uncertainties to the test flow condition. A shock-expansion tube (SET) has the potential to mitigate the aforementioned concerns to a certain extent and generate relatively steady and clean test gas of really high enthalpy. A SET, named JF-16, has been built at the State Key Laboratory of High Gas Dynamics (LHD) and has successfully generated hypervelocity test flows up to 8 kmps. However, the test duration of a SET is extremely shorter as compared to a RST of the same scale which results in difficulties in the measurements and diagnostics. It is an applicable means to use CFD techniques, coupled with available experimental measurement, to determine the characteristic of the test flow in a SET.

The dispersion-controlled dissipative scheme (DCD) was proposed by Jiang et al [1,2]. The scheme has been applied in our group and been working well for the simulation of chemically non-equilibrium flows [3-5], especially with the presence of strong shock waves [6-11]. The DCD scheme is smart to adjust numerical viscosity by itself according to the simulated flow problem to maintain numerical stability without any pre-posed parameters. Figure 1 shows the comparison of TVD scheme [12] and DCD scheme for the computations of Mach reflection of oblique shock waves in Ma=4 supersonic flow. Numerical instability, the carbuncle phenomenon, occurs at the Mach stem as depicted in (a) and (b). Increasing the entropy correction parameter, δ, of the TVD scheme can mitigate the carbuncle and may eliminate it when δ=0.5. On the contrary, the DCD

* Corresponding author: huzm@imech.ac.cn

scheme is robust enough to give a correction Mach reflection solution as depicted in (c) without any adjustable parameter.

In this paper, the DCD scheme is used to setup our SET simulation code. Several numerical issues rising in our preliminary investigation are discussed, which include the initial shock structure under the background of chemical non-equilibrium and spurious oscillation. A new flux splitting algorithm based on local characteristics is worked out for the DCD scheme to improve the numerical stability. Then, the updated algorithm is used to compute several hypervelocity test cases that have been conducted recently in the lab of LHD.

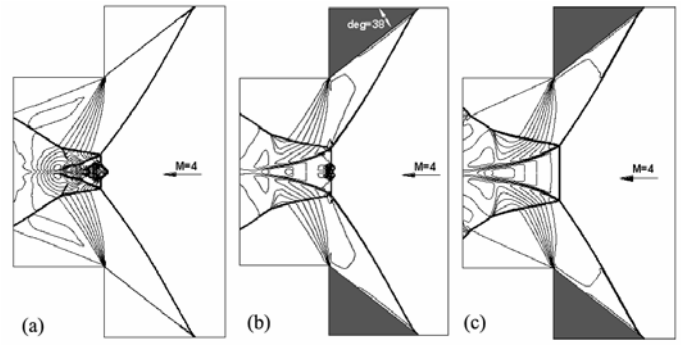

Fig. 1 Mach reflection simulated with TVD and DCD scheme, respectively, (a) TVD scheme with entropy correction parameter δ=0.15; (b) TVD scheme with δ=0.25; (c) DCD scheme

2. Flux splitting algorithm for the DCD scheme

In the current investigation, the Euler system for multi-component reactive gaseous mixture is used as the governing equations. Details about the equations and the original DCD scheme for reactive flows may be found in our previous work [3,6]. The original DCD [1,2] scheme is of the flux vector splitting family where the numerical flux at the cell interface 'i+1/2' is written as:

$$F_{i+1/2}^{SWs} = F_i^{+} + F_{i+1}^{-} + 0.5\min\bmod(F_i^{+} - F_{i-1}^{+}, F_{i+1}^{+} - F_i^{+}) - 0.5\min\bmod(F_{i+1}^{-} - F_i^{-}, F_{i+2}^{-} - F_{i+1}^{-}). \quad (1)$$

Here, the split flux at four nodes as depicted in Fig. 2(a), i.e., i-1, i, i+1, i+2 are need which can be obtained using Steger-Warming algorithm [13].

$$F_j^{\pm} = \frac{\rho}{2\hat{\gamma}} \begin{bmatrix} C_1\left[2(\hat{\gamma}-1)\lambda_1^{\pm} + \lambda_{ns+2}^{\pm} + \lambda_{ns+3}^{\pm}\right] \\ C_2\left[2(\hat{\gamma}-1)\lambda_1^{\pm} + \lambda_{ns+2}^{\pm} + \lambda_{ns+3}^{\pm}\right] \\ \vdots \\ C_{ns}\left[2(\hat{\gamma}-1)\lambda_1^{\pm} + \lambda_{ns+2}^{\pm} + \lambda_{ns+3}^{\pm}\right] \\ u\left[2(\hat{\gamma}-1)\lambda_1^{\pm}\right] + (u-a)\lambda_{ns+2}^{\pm} + (u+a)\lambda_{ns+3}^{\pm} \\ v\left[2(\hat{\gamma}-1)\lambda_1^{\pm} + \lambda_{ns+2}^{\pm} + \lambda_{ns+3}^{\pm}\right] \\ 2\left[(\hat{\gamma}-1)H - a^2\right]\lambda_1^{\pm} + (H-au)\lambda_{ns+2}^{\pm} + (H+au)\lambda_{ns+3}^{\pm} \end{bmatrix} \quad (2)$$

$$(j = i-1, i, i+1, i+2)$$

For a multi-component Euler system, the Steger-Warming algorithm gives a very simple and symmetric flux [3, 6] as re-written in eq.(2). The code employing the original DCD scheme is sufficiently robust and efficient for applications in the fields of detonation [5, 7, 8, 9], high-power chemical laser [3, 4] and hypersonic shock physics [10, 11]. As can be seen in Fig. 2(a), the split flux at nodes i-1, i, i+1and i+2 are calculated based the characteristic parameters at each node. However, computational tests show spurious oscillation, which will be

given in the following section, if the original algorithm is applied for the SET hypervelocity flow of JF-16. Therefore, a modification to the scheme is worked out as written in eq. (3). Here, the intermediate flux at each node uses the same characteristic parameters at the cell interface 'i+1/2', see Fig. 2(b). The numerical flux shall be calculated by matrix operation and the simple form of Eq. (2) is not applicable. As such, the modified DCD scheme is more time-consuming than the original. The details of the symbols in above equations may be found in the previous work [3, 6].

$$F_{i+1/2}^{SWm} = R_{i+1/2}[f_i^+ + f_{i+1}^- + 0.5\min\text{mod}(f_i^+ - f_{i-1}^+, f_{i+1}^+ - f_i^+) - 0.5\min\text{mod}(f_{i+1}^- - f_i^-, f_{i+2}^- - f_{i+1}^-)] \quad (3)$$

$$f_j^{\pm} = (\Lambda^{\pm}L)_{i+1/2}U_j \ , (j = i-1, i, i+1, i+2) \quad (4)$$

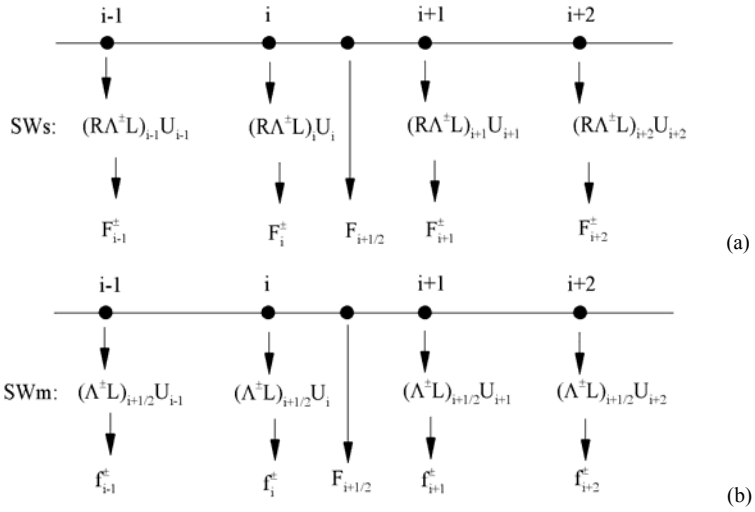

Fig. 2 Sketch of the flux splitting algorithms for (a) the original DCD scheme (DCD-SWs) and (b) the updated DCD scheme (DCD-SWm)

3. Test flow condition of JF-16

3.1. Numerical setup

The configurations of geometry and wave process of the shock-expansion tube JF-16 is schematically shown in Fig. 3. There are two diaphragms which divide the facility into three sections, i.e., the detonation tube, shock tune and accelerating tube. After the detonation wave breaking the diaphragm I, the primary shock wave (psw) is generated in the shock tube followed by the primary contact surface (pcs) that separates the driver gases and the driven gas. In a reflected shock tunnel (RST), the driven as is stagnated at the nozzle which results in erosion and contamination due to the high temperature. On the contrary, the psw along with the driven gas in a SET moves downstream into the accelerating tube after breaking the diaphragm II. Through the unsteady expansion (ue) the driven gas is further accelerated to generate the test gas in the Zone #5. This is the working mechanism of the JF-16 SET.

For the test condition at the total enthalpy of around 45 MJ/kg, the Mach number of psw wave in the shock tube and secondary shock wave (ssw) in the expansion tube is around M_{psw}=13.9 and M_{ssw}=27, respectively. The static temperature is sufficiently high to cause dissociation of oxygen (post-shock of psw) and nitrogen (post-shock of ssw), respectively. As such, a chemical reaction model as listed in Table 1 should be applied in the present computations. The model consists of seventeen elementary reactions among five species, i.e., N_2, O_2, NO, O and N, while ionization is not considered here.

For simplicity, only a part of the shock tube and acceleration tube as shown in the dashed-box in Fig. 3 are simulated. Therefore, the incident shock wave, i.e., psw, in the shock tube should be predetermined for the initial condition. Measurement and diagnostics, as aforementioned, are challenging in a SET due to the extremely short test time. Fortunately, the shock speed measured by ionization probes, e.g., V_{psw}=4823 m/s (corresponding to M_{psw}=13.9), is applicable and reliable especially for strong shock waves. The shock tube and acceleration tube are initially filled with air at temperature, T_1=T_7=300 K, and pressure p_1=30 mmHg and p_7= 0.1 mmHg, respectively.

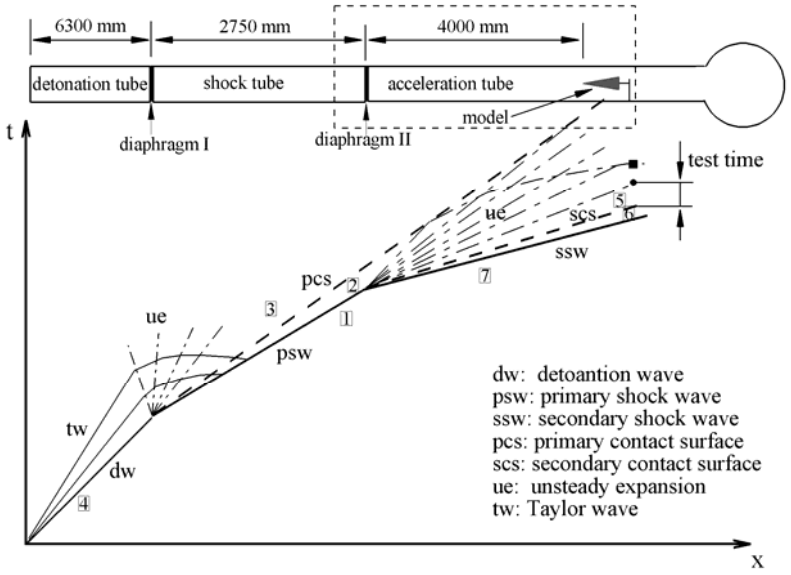

Fig .3 Sketch of the configuration and wave graph for JF-16 shock-expansion tube,(the dashed-box is the computational domain)

Table 1 Reaction model of air (five species: N_2, O_2, NO, O, N)

No.	Reaction equation	A	n	Ea
1	O_2+N=O+O+N	1.0×10^{22}	-1.5	118469
2	O_2+O=O+O+O	1.0×10^{22}	-1.5	118469
3	O_2+ N_2=O+O+N_2	2.0×10^{21}	-1.5	118469
4	O_2+ O_2=O+O+O_2	2.0×10^{21}	-1.5	118469
5	O_2+NO=O+O+NO	2.0×10^{21}	-1.5	118469
6	N_2+N=N+N+N	3.0×10^{22}	-1.6	225167
7	N_2+O=N+N+O	3.0×10^{22}	-1.6	225167
8	N_2+N_2=N+N+N_2	7.0×10^{21}	-1.6	225167
9	N_2+O_2=N+N+O_2	7.0×10^{21}	-1.6	225167
10	N_2+NO=N+N+NO	7.0×10^{21}	-1.6	225167
11	NO+N=N+O+N	1.1×10^{17}	0.0	150167
12	NO+O=N+O+O	1.1×10^{17}	0.0	150167
13	NO+N_2=N+O+N_2	5.0×10^{15}	0.0	150167
14	NO+O_2=N+O+O_2	5.0×10^{15}	0.0	150167
15	NO+NO=N+O+NO	1.1×10^{17}	0.0	150167
16	N_2+O=N+NO	1.8×10^{14}	0.0	76132
17	O+NO= O_2+N	6.9×10^{8}	1.1	38181

Note: (1) Unit: mole, s, cm, K, cal, (2) Arrhenius mass generation rate: $k_f = AT^n e^{-Ea/RT}$

3.2. Incident shock structure under the background of chemical non-equilibrium

As aforementioned, the primary shock wave is pre-determined via the measured shock speed as the initial condition. For a shock wave in an inert gas flow, a sharp jump, of each flow variable is consistent and applicable. Such a methodology, however, doesn't work well the current problem because of the chemical reaction (see Table 1) following the shock wave, psw. If the sharp jump condition is straightforwardly used, bumps will be generated post psw as shown in Fig. 4(a) due to the mismatched initial conditions. Such bumps will result in spurious oscillation at the head of the unsteady expansion (ue) fan as shown in Fig. 4(b). The reason is that the shock front structure in chemically reactive flow is no longer a simple jump as that in an inert gas flow. Instead, a pulse-shaped front for the temperature profile as shown in the dashed box in Fig. 4(a) is consistent with the chemical non-equilibrium process according to the chemical kinetics given in Table 1. With such an initial structure of psw, the spurious oscillation can be cleared away and the correct profiles, e.g., of pressure and density, will be put in the figures the in following sections. Of course, the front structure of psw is obtained from a separate running and copied as the final initial conditions.

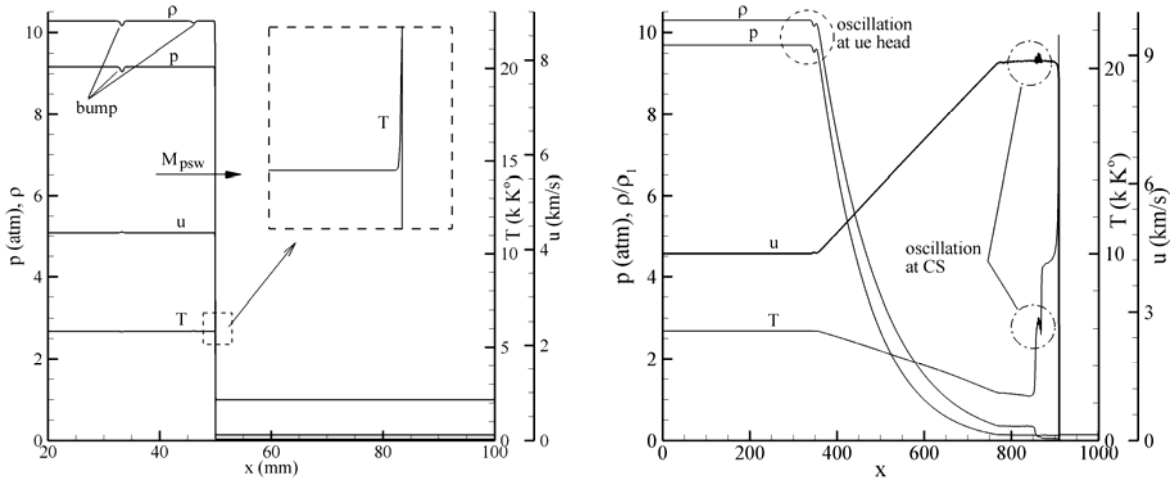

Fig .4 Structure of the primary shock wave for the initial setup (a) and spurious oscillation (b), the original DCD scheme, i.e., DCD-SWs is used in the computation.

3.3. Spurious oscillation at the secondary contact surface

In Fig. 4(b), one can also see spurious oscillations in the velocity and temperature profiles at the contact surface where the DCD-SWs scheme as given in eqs. (1-2) and depicted in Fig. 2(a) is used. Why the scheme works well in a lot of previous applications [3-11] but leads to spurious oscillation in the present work? Through a series of troubleshooting tests, an updated scheme as named DCD-SWm which is defined in eqs. (3-4) and illustrated in Fig. 2(b) can eliminate the aforementioned numerical instability at scs. The calculated profiles for hypervelocity flow of total enthalpy of 45 MJ along with the species are depicted in Fig. 5 where we cannot see spurious oscillation in the vicinity of scs any more. Of course, the oscillation at the ue head is also eliminated when the consistent initial condition as aforementioned for the incident shock wave, psw, is imposed.

We can find that a test flow, the zone (5) as shown in Fig. 5 (a), of super-orbital speed, 8850 m/s is obtained in the SET of JF-16. This corresponds to a shock speed of 9500 m/s which is about ten percent higher than the experimental measurement. Such a discrepancy is reasonable as the viscous effect is not considered in the

present simulation. The shock-tube attenuation is around 3% per meter [14] according to a tread deal of experimental studies and empirical analysis. In the current study, the distance from diaphragm to the test section is 4 meters long. Therefore, the viscous effect may cause 12% attenuation which may accounts for the aforementioned discrepancy.

Figure 5(b) show the profile of mole fraction for each species at the transient when the ssw arrives at the test windows. We can find that the test gas primarily consists of molecular nitrogen and atomic oxygen, i.e., N_2 and O, which is a discrepancy between the obtained test flow and the real high-enthalpy flight condition. This is due to the high temperature, T_5=2665 K, of the test flow as shown in Fig. 5(a). Therefore, further expansion via a diverging tube is recommended to JF-16 to cool down the test flow. From Fig. 5(b) we can also find that molecular nitrogen is almost completely dissociated in the shocked accelerating gas, zone (6) because of the extremely high temperature of around 9337 K.

From the current simulation, it is found that the duration of the test flow of JF-16 is around 60μs while duration the accelerating gas flow is around 30μs. The short test time cause difficulties in diagnostics and measurements for the temperature and pressure.

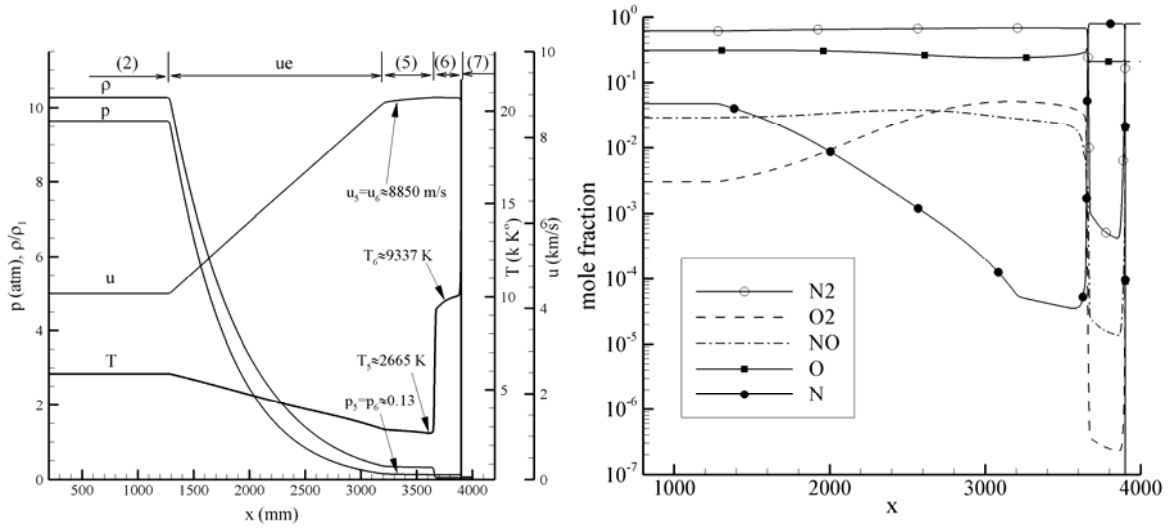

(a) (b)

Fig .5 Profiles of flow variables in the shock-expansion tube (a) and species distribution (b), the updated DCD scheme, i.e., DCD-SWm is used in the computation.

3.4. Hypervelocity flow tests

The flow zones for different conditions are labeled in Fig. 3 as well as Fig. 5(a) while the flow parameters for zone (5) and (6) are listed in Table 2. With the numerically obtained data of the test flow reasonably agree with experiments, further computations are conducted for the hypervelocity flow over several test models such as wedge, cone and double-cone. The comparison for each is shown in Fig. 6. Here, the experiment is imaged for the self-illumination of the main species while the original intention is schlieren. The shock shapes obtained by experiments and computations, respectively, agree with each other which can lead to mutual confirmation of the numerical and experimental tests for JF-16.

One of the interesting findings should be noted that the images shown in Fig. 6(c1) and (c2) indicate that the high brightness over the second cone of the double-cone model is self-illumination of atomic nitrogen. Distribution of each species for others, such as N_2, O_2, NO and O doesn't agree with the experiment, respectively.

It is reasonable that the molecular nitrogen may be partly dissociated because of the high temperature post the oblique shock wave originating from the corner of the double-cone model.

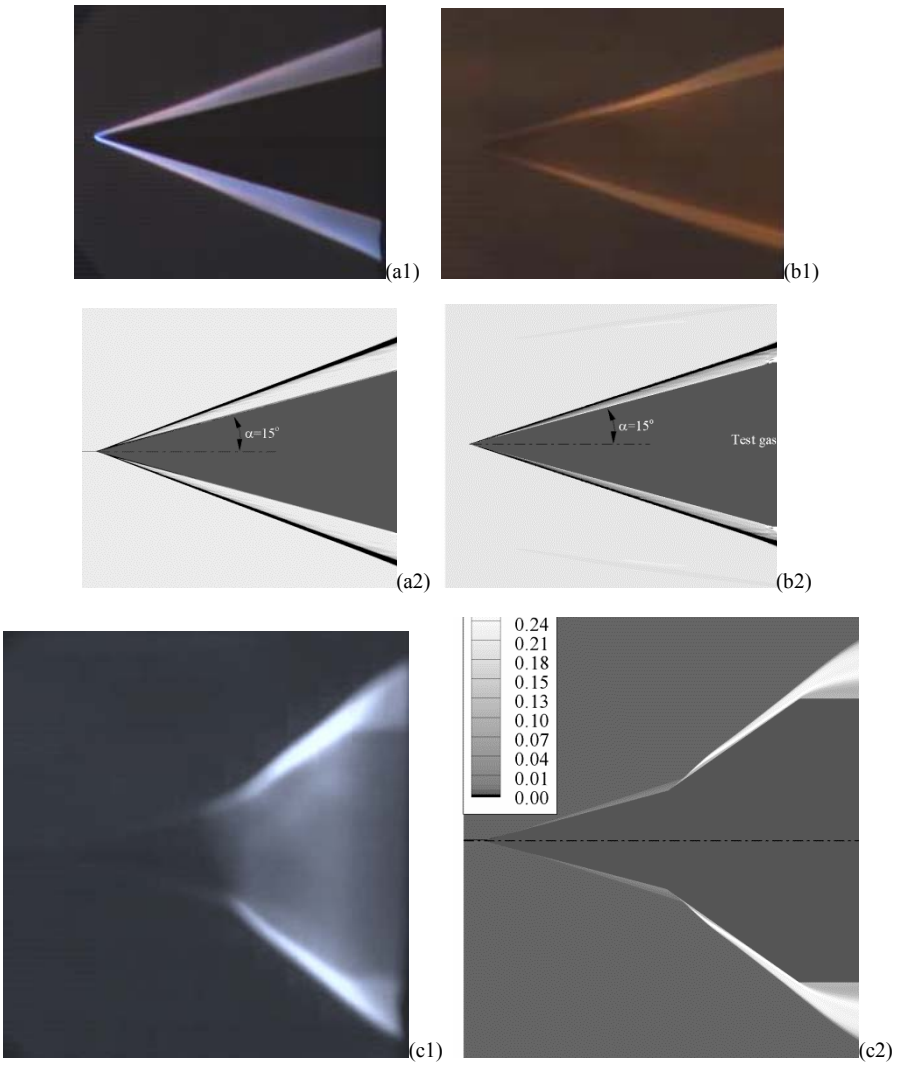

Fig .6 Hypervelocity test and corresponding computations: (a1) experiment and (a2) numerical schlieren for a wedge with half angle of 15°; (b1) experiment and (b2) numerical schlieren for a cone with half angle of 15°; (c1) experiment and (c2) numerical density contour of N for a double-cone with half angles of 15°+35°.

Table 2 Test flow condition of JF-16 at 45 MJ

Zone	Mole fraction					T (K)	P (atm)	V (m/s)	Ma
	N_2	O_2	NO	O	N				
Test gas	0.675	0.039	0.019	0.266	1.0e-5	2665	0.13	8850	8.2
Accelerating gas	4.8e-4	1.0e-7	1.0e-5	0.21	0.7894	9337	0.13	8930	3.2

4. Conclusions

In the present study, the dispersion-controlled-dissipative scheme (DCD) is updated to eliminate the spurious oscillation for the simulation of hypervelocity flows in the shock-expansion tube (SET), JF-16. Numerical instabilities, when the original DCD scheme is applied for the interested problem, occur at the contact surface, where strong discontinuities in flow parameters exist. The computation is validated by the shock speed measured in experiment via ionization probes. Further computations for several test models agree with the experimental visualization. In addition, the flow visualization of double-cone test is found to be the self-illumination of atomic nitrogen by comparing to the numerical output.

Acknowledgement

The author Hu ZM was supported by NSFC under the grant No. 11142006 and the Youth Innovation Fund (2011) from the State Key Laboratory of High Temperature Gas Dynamics, Institute of Mechanics, CAS.

References

[1] Jiang, Z.L., Takayama, K., Chen, Y.S. Dispersion conditions for non-oscillatory shock-capturing schemes and its applications. Comput. Fluid Dyn. J. 2 (1995)137–150 .

[2] Jiang, Z.L. On the dispersion-controlled principles for non-oscillatory shock-capturing schemes. Acta Mech. Sin. 20(1) (2004) 1–15.

[3] Hu Z.M., Lü J.M., Jiang Z.L., Myong R.S., Cho T.H. Numerical study on the off-design/on-design performance of nozzle flow for supersonic chemical oxygen-iodine lasers. Acta Mech. Sin. 24(2) (2008) 133-142.

[4] Hu Z.M., Jiang Z.L., Myong R.S., Cho T.H. Numerical analysis of spatial evolution of the small signal gain in a chemical oxygen-iodine laser operating without primary buffer gas. Opt Laser Tech. 40(1) (2008) 13-20.

[5] Hu Z.M. and Jiang Z.L. Wave Dynamic process in cellular detonation reflection from wedges. Acta Mech. Sin. 23(1) (2007) 33-41.

[6] Hu Z.M., Myong R.S., Cho T.H. A robust scheme for the multi-component reactive flows in the presence of shock waves. The Korean Society of Computational Fluid Engineering, 12(1):60-67, 2007.

[7] Teng H.H., Jiang Z.L. and Hu Z.M. Detonation initiation developing from the Richtmyer-Meshkov instability. Acta Mech. Sin. 23(4) (2007) 343-349.

[8] Deng B., Hu Z.M., Teng H.H. and Jiang Z.L. Numerical study on cellular structure evolution of detonation in section-changing chambers. Science in China Series G 50(6) (2007) 797-808.

[9] Hu Z.M., Dou H.S., Khoo B.C. Rapid detonation initiation by sparks in a short duct: a numerical study. Shock Waves 20 (2010) 241-249.

[10] Hu, Z.M., Myong, R.S., Kim, M.S., Cho, T.H.: Downstream flow conditions effects on the RR→MR transition of asymmetric shock waves in steady flows. J. Fluid Mech. 620 (2009) 43–62

[11] Hu, Z.M., Wang, C., Zhang, Y., Myong, R.S.: Computational confirmation of an abnormal Mach reflection wave configuration. Phys. Fluids 21 (2009) 011701.

[12] Yee H.C., Klopeer G.H. Montagne J.L. High-resolution shock-capturing scheme for inviscid and viscous hypersonic flows. J. Compt. Phys. 88 (1990) 31-61.

[13] Steger, J.L.,Warming, R.F.: Flux vector splitting of the inviscid gas dynamic equations with applications to finite difference method. J. Computat. Phys. 40 (1981) 263–293.

[14] Spence D.A., Woods A. A review of theoretical treatment of shock-tube attenuation. J. Fluid Mech. 19(2) (1964) 161-174.